

# AN OPTICAL FIBRE BLM SYSTEM AT THE AUSTRALIAN SYNCHROTRON LIGHT SOURCE

M. Kastriotou\*<sup>1,2</sup>, E.B. Holzer, E. Nebot del Busto<sup>1,2</sup>, CERN, Geneva, Switzerland

<sup>1</sup> also at University of Liverpool, Liverpool, UK

<sup>2</sup> also at Cockcroft Institute, Warrington, UK

C.P. Welsch, Cockcroft Institute, Warrington; University of Liverpool, UK

M. Boland, SLSA, Clayton, Australia; University of Melbourne, Australia

## Abstract

Increasing demands on high energy accelerators are triggering R&D into improved beam loss monitors with a high sensitivity and dynamic range and the potential to efficiently protect the machine over its entire length. Optical fibre beam loss monitors (OBLMs) are based on the detection of Cherenkov radiation from high energy charged particles. Bearing the advantage of covering more than 100 m of an accelerator with only one detector and being insensitive to X-rays, OBLMs are ideal for electron machines.

The Australian Synchrotron comprises an 100 MeV 15 m long linac, an 130 m circumference booster synchrotron and a 3 GeV, 216 m circumference electron storage ring. The entire facility was successfully covered with four OBLMs. This contribution summarises a variety of measurements performed with OBLMs at the Australian Synchrotron, including beam loss measurements during the full booster and measurements of steady-state losses in the storage ring. Different photosensors, namely Silicon Photo Multipliers (SiPM) and fast Photo Multiplier Tubes (PMTs) have been used and their respective performance limits are discussed.

## INTRODUCTION

Optical fibre beam loss monitors comprise an optical fibre coupled to a photosensor. Their operation principle is the detection by the photosensor, of Cherenkov photons [1], which are generated in the fibre by high energy charged particles produced through a beam loss. With the advantages of covering long distances while being sensitive to electrons and insensitive to X-rays, these monitors can be favorable for the machine protection of light sources.

The position reconstruction of OBLMs for electron storage rings has been discussed in past studies [2]. In the present paper the potential of covering the complete machine and the performance of OBLMs during normal operation of a light source is examined at the Australian Synchrotron Light Source.

## EXPERIMENTAL SETUP

### *The Australian Synchrotron*

In the Australian Synchrotron [3], electrons are generated in a 500 MHz thermionic gun and enter a 15 m linac, which

accelerates them to 100 MeV. The electrons are then injected into a 130 m booster ring that further accelerates them up to 3 GeV. During the last few tens of milliseconds of the 600 milliseconds ramping cycle, the closed orbit is altered via a slow bumping technique. This allows the beam to be centered at the extraction point within the field of the fast magnet that kicks the beam into the Beam To Storage ring (BTS) transfer line. At the end of the BTS, another kicker magnet injects the beam into Sector 1 of a 216 m circular storage ring that consists of 14 sectors with a double bend achromat lattice. Sector 11 contains the beam scrapers used to concentrate the beam losses at this location and so protect the multiple insertion devices located elsewhere in the ring.

During standard operation, the storage ring holds a beam current of 200 mA, injected in trains of 75 bunches and a current of approximately 0.5 mA. Nominally, the beam fills 300 out of the 320 available 500 MHz buckets. Beam lifetimes as good as 200 hours can be reached. When operating in single bunch mode, the bunch charge can be varied in the range of  $10^{+5} - 10^{+9}$  electrons [4].

### *Installation*

The entire accelerator complex of the Australian Synchrotron Light Source was covered for the observation of beam losses with a set of only four optical fibres. Each fibre consists of a 200  $\mu\text{m}$  pure silica core, 245  $\mu\text{m}$  cladding and a 345  $\mu\text{m}$  acrylate coating. A dark nylon jacket provides protection against ambient light and mechanical breakage.

The schematic of the installed cables and their respective photon sensors is shown in Fig. 1. Two fibres were installed symmetrically on the inner and outer side of the linac, each covering half of the booster ring. One of these also covered a large fraction of the BTS transfer line as well as the booster extraction point. Only one optical end of each of these fibres is extracted to the roof of the facility, at Sector 2. The other two fibres cover half of the storage ring, each with photosensors installed in both ends [2].

### *Photosensors*

Two types of photosensors have been examined in the present study: A Hamamatsu fast photomultiplier tube (H10721-10) and a Silicon Photomultiplier (Multi Pixel Photon Counter S12572-015C) [5]. The latter is coupled to a transimpedance amplifier (comprised of a Texas Instruments THS3061 operational amplifier [6] and a feedback resistor)

\* maria.kastriotou@cern.ch

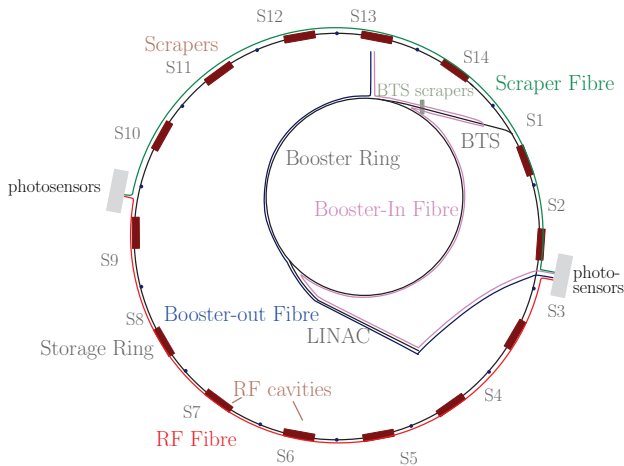


Figure 1: A sketch of the four optical fibre BLMs installed at the Australian Synchrotron Light Source. The Scrapper fibre (green) and the RF fibre (red) cover the Storage Ring, the Booster-In fibre (magenta) covers the linac and half the booster ring, while the Booster-out fibre (blue) covers the linac, half of the booster ring and the BTS line.

enclosed in a custom made RF shielded module with low pass filters in the bias input to reduce noise as described in [7]. The back-end electronics for the acquisition of the signals are described in detail in [2].

### STEADY-STATE LOSSES

#### Method

Two beam losses scenarios were studied during the injection of electrons into the storage ring. In the first case injection losses were studied by injecting single bunches into the storage ring, with beam already circulating and the beam scrapers entirely open. In the second case, nominal 75 bunch trains were injected into a previously empty storage ring, with the beam scrapers positioned to leave an 11 mm gap.

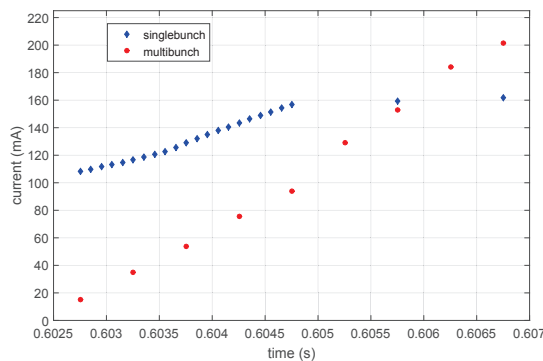


Figure 2: Circulating beam in the storage ring after each set of 50 shots in the single bunch and 25 shots in the multi bunch case, with respect to the trigger timing.

Table 1: Experimental Cases Studied

bunches	Scrapers	sample interval	time window
1	open	1 ns	56 000 ns
75	nominal	10 ns	500 000 ns

The data presented here were collected at Sector 2, from the downstream of the scrapper fibre using the fast-PMT and the upstream of the RF fibre via the SiPM (channel A and B respectively). As the data acquisition depth was limited to 56  $\mu$ s (single bunch case) and 500  $\mu$ s (multi bunch case), to look at losses at later times the trigger time was delayed. For each trigger timing, 50 shots with 56000 samples and 1 GHz sampling rate were taken in the case of single bunch injections, whereas in the multi bunch case 25 shots with 50000 samples and 0.1 GHz sampling rate were acquired. The characteristics of the two different measurements are summarised in Table 1. Fig. 2 shows the beam current after each number of datasets acquired per trigger timing, as measured by the beam current monitor of the storage ring for the two cases.

Since steady-state losses are expected to be on the order of a few electrons per turn, an estimation of the OBLM background for such a measurement is essential. Without beam in the machine 30 background datasets were acquired and the mean value of the signals obtained is presented in Fig. 3. To ensure that the signals detected in the steady-state case were real beam losses, a value greater than the maximum of the background signals was considered as a cutoff value, with  $V_{cut} = 0.0006$  V for channel A and  $V_{cut} = 0.0137$  V for channel B. These background signals are attributed mainly to the photosensors, and the difference between them comes from their different noise levels. In the case of the SiPM, an offset is also introduced by the transimpedance amplifier front end electronics.

The detected charge (charge that the photosensor generates) for the PMT was calculated from all samples whose

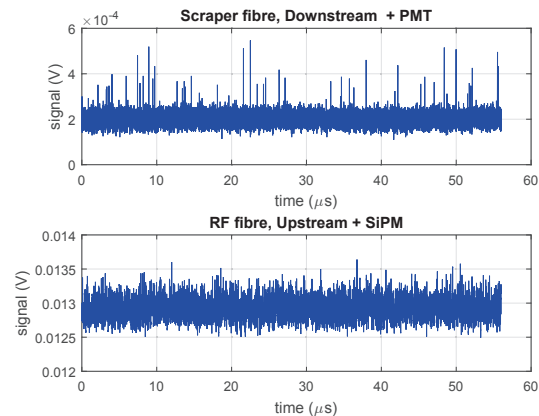


Figure 3: Background of the fibres covering the storage ring.

value was higher than the selected cutoff, as:

$$C_{PMT} = \frac{\sum (V - V_{off})_{(V > V_{cut})} \times t}{R}, \quad (1)$$

where  $R = 50 \Omega$  the measurement load and  $t$  is the sample interval. The signal offset  $V_{off}$  has been estimated as the mean value of the background signal. For the SiPM with the transimpedance amplifier readout, the respective value for the generated charge has been calculated as:

$$C_{SiPM} = \frac{2 \times \sum (V - V_{off})_{(V > V_{cut})} \times t}{R_F}, \quad (2)$$

where  $R_F = 0.5 \text{ k}\Omega$  is the feedback resistor.

Due to the different time windows and in order to compare the two cases, the detected current was estimated as  $I_{sb} = C_{sb}/56000 \text{ (A)}$  and  $I_{mb} = C_{mb}/500000 \text{ (A)}$  for the single bunch and the multi bunch case respectively.

## Results

A comparison of the two measurements is summarised in Fig. 4. Each point corresponds to the mean value of the

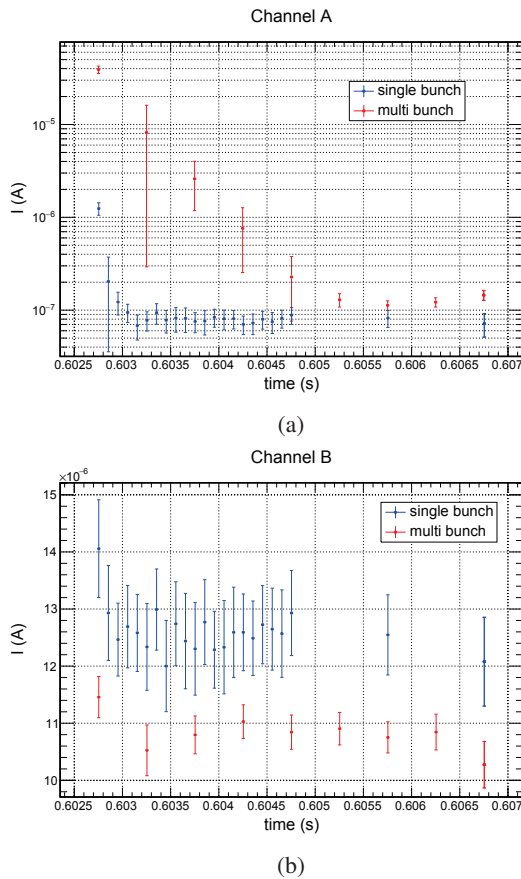


Figure 4: Comparison of the detected current in the single bunch and the multi bunch case. (a) For Channel A, with a fast PMT coupled to the downstream of the Scraper fibre. (b) For Channel B, with an SiPM coupled to the upstream of the RF fibre.

signal for the number of datasets acquired per trigger timing. In Fig. 4a, the signals of the Scraper fibre downstream end, coupled to the PMT, are presented. In both cases the exponential loss decay, which is characteristic of the beam injection process, can be observed. During this time the losses measured for the multi bunch (scrapers in) case are up to two orders of magnitude higher than the ones of the single bunch case (scrapers out), which is attributed both to the larger beam charge and the presence of scrapers. When reaching the steady-state the signals of the multi bunch are slightly higher, again probably due to the higher charge and beam cleaning at the scrapers. Figure 4b, shows the signals of the RF fibre upstream end connected to the SiPM. In this case, losses at injection are not observable. However, the single bunch case shows losses constantly higher than in the multi bunch case, when the beam has been cleaned before, which indicates the detection of steady-state losses by the OBLMs.

## BEAM LOSSES DURING THE BOOSTER CYCLE

### Method

The beam losses during the complete booster cycle of the Australian Synchrotron, from the beam injection to the extraction through the BTS to the Storage Ring, have been measured with the installed OBLMs.

For this study the Booster-In fibre was connected to the fast-PMT and the Booster-Out fibre to the SiPM. The fiber background, i.e. the signal measurement in absence of circulating beam, estimated as an average of 30 shots is presented in Fig. 5. The booster background signals are very similar to the ones observed for the storage ring (Fig. 3), which points to the noise coming mainly from the photosensors themselves. A value of  $V_{cut} = 0.00036 \text{ V}$  was considered as an offset for the Booster-In fibre and the PMT, and of  $V_{cut} = 0.0134 \text{ V}$  for the Booster-Out fibre and the SiPM. As above, different times of the booster cycle are explored by delaying the trigger time. For each point 50 shots were

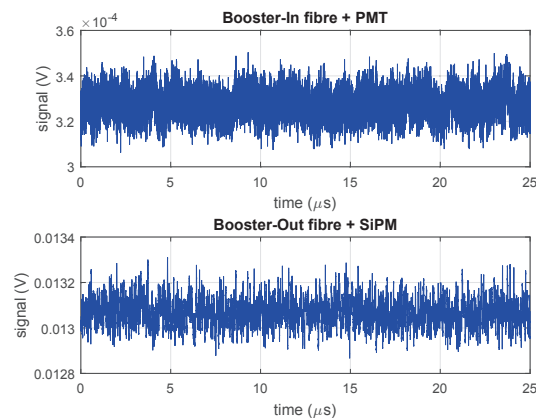


Figure 5: Background of the two fibres covering the Linac, Booster and BTS line.

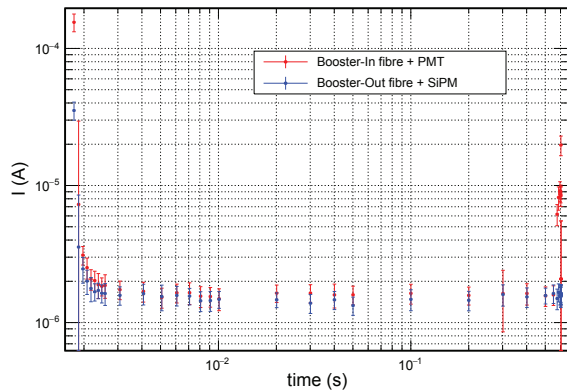


Figure 6: Beam losses during the booster cycle as detected by the Booster-In fibre coupled to a fast-PMT, and the Booster-Out fibre coupled to an SiPM. Due to the different gain of the photosensors, the two signals can only be compared qualitatively and not quantitatively.

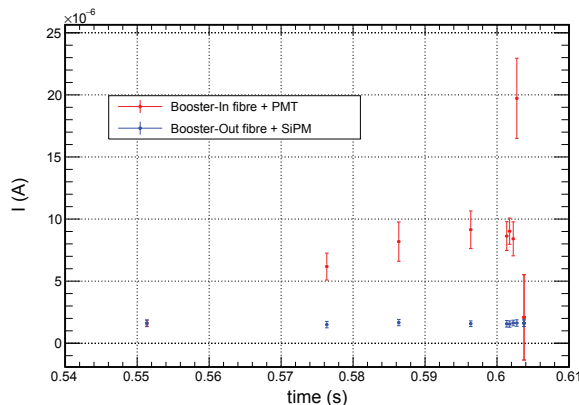


Figure 7: Losses during the last milliseconds of the booster cycle before extraction to the storage ring (zoom of Fig. 6).

acquired, with 1 GHz sampling rate and 25000 samples. The charge collected by the photon sensors was estimated via Eq. (1) and (2) for the PMT and SiPM respectively. For consistency with the previous results, the detected current was calculated as  $I = C/25000$  (A).

### Results

Figure 6 shows the signals detected by the two booster fibres throughout the full cycle. The injection into the booster is rather noticeable with detected charges that reach up to  $100 \mu\text{A}$ . In the following milliseconds, an exponential decay characteristic of the injection process is observed. After the first 4 ms the losses reach a plateau compatible with zero signal. However, the signals observed on the plateau are

consistently higher than the range of dark current expected for the two photon sensors, namely: 1 nA for the fast PMT and 100 nA for the SiPM.

The beam extraction to the storage ring is illustrated in higher detail on Fig. 7. A gradual increase of the losses in the case of the Booster-In fibre can be observed, which is attributed to losses developed in the BTS line, a location covered only by this fibre. The losses increase further as the beam is injected to the storage ring and after the injection decrease to the value of the plateau. In the Booster-Out fibre the extraction losses cannot be observed. This is due to the fact that this particular fibre does not cover the BTS line region.

## CONCLUSION

Optical fibre BLMs have been installed and tested for their performance at the Australian Synchrotron Light Source facility. It has been demonstrated that OBLMs are capable of detecting losses during beam injection to the storage ring, and that they have the capability of detecting steady-state losses. Two photosensors, a fast-PMT and an SiPM, were examined showing similar behaviour. The main difference between the two detectors is their noise levels, and the higher noise of the SiPM may render the detection of very low signals more challenging.

## ACKNOWLEDGMENT

The authors of this paper would like to thank the operators of the Australian Synchrotron Light Source for their invaluable help on the execution of the experiments. This work has been partly funded by the Royal Society via the International Exchange Scheme project PPR10353.

## REFERENCES

- [1] Jelley, J. V., "Čerenkov Radiation and its Applications", 1958, Pergamon Press, London
- [2] E. Nebot del Busto et al., "Position resolution of optical fibre-based beam loss monitors using long electron pulses", IBIC' 15, Melbourne, September 2015, WECLA03
- [3] J. Boldeman et al., "The physics design of the Australian Synchrotron Storage Ring", Nucl. Instr. and Meth., A 521, 2004
- [4] E. Nebot del Busto et al., "Measurement of Beam Losses at the Australian Synchrotron", IBIC' 14, Monterey, September 2014, WECZB3
- [5] Hamamatsu Photonics K.K., <http://www.hamamatsu.com/>
- [6] Texas Instruments Inc., <http://www.ti.com/>
- [7] M. Kastriotou et al., "A Versatile Beam Loss Monitoring System for CLIC", IPAC' 16, Busan, May 2016, MOPMR024